Electronic structure of transition-metal impurities in copper

P. Blaha and J. Callaway
Department of Physics, Louisiana State University, Baton Rouge, Louisiana 70803
(Received 13 June 1985)

The electronic structure of magnetic transition-metal impurities (Fe,Co,Ni) in Cu is calculated by means of a cluster approach and the local-spin-density approximation. The wave functions were expanded into Gaussians and no shape approximation to the potential was made. We report the results of the energy-level distribution in 13-atom fcc clusters of Cu_{13}, $Cu_{12}Fe$, and in 19-atom clusters ($MCu_{12}Cu_6$, M=Cu,Fe,Co,Ni) which are in strong disagreement with $X\alpha$ scattered-wave results. The local cluster density of states (DOS) agrees very well with the respective bulk and surface DOS of Cu metal. For the Fe impurity we obtain a local moment of $3.05\mu_B$, which is in good agreement with experiment and Green's-function calculations. The spin densities show, besides the strong localized Fe moment, a negative polarization of the conduction electrons as indicated by a Mulliken population analysis or direct examination of the spin densities in the (100) plane. Previous observations of scattering in de Haas–van Alphen experiments, which showed that mainly spin-down states are involved, are in agreement with our local DOS. For the Co and Ni systems the impurity moment is reduced to $2.05\mu_B$ and $0.69\mu_B$; however, the Ni impurity might become nonmagnetic by including more Cu shells or proper boundaries in the calculation. This is indicated through the level distribution as well as the high correlation of magnetism in both Cu shells.

I. INTRODUCTION

Our understanding of the electronic structure of ideal solids has increased steadily in recent years. This progress has been achieved mainly due to improvements in local-density-functional theory and better and more accurate band-structure calculational methods. However, nature normally does not build such ideal systems, and very often isolated impurities in an otherwise more or less ideal crystal modify drastically the microscopic and macroscopic properties of these solids.

Much experimental and theoretical research has been done in regard to dilute systems of transition-metal impurities alloyed in otherwise nonmagnetic metals. These systems, sometimes also forming spin glasses with increased concentration, are often called "Kondo systems" and have been investigated by many authors. Common models describing the magnetic properties are the (i) virtual-impurity-state model and the (ii) impurity-ion crystal-field model.[1,2] Concepts like the "Kondo compensation cloud" or localized spin fluctuations are widely used.

We are concerned here with first-principles calculations of the electronic structure of such systems on the basis of density-functional theory. Previous calculations have been of two types: calculations for finite clusters and Green's-function calculations for impurities embedded in the bulk solid. Johnson, Vvedensky, and Messmer[3] performed $X\alpha$ scattered-wave cluster calculations for several of these impurity systems. Their results are in complete disagreement with later Green's-function impurity calculations by Zeller, Dederichs, and co-workers.[4–7] The latter authors argued that the cluster approach is unsuitable for the description of impurities in solids. However, in spite of major conceptual differences between bulk solids and small clusters (in contrast to a cluster, a bulk metal has a sharp Fermi surface, and excitations across it can occur with vanishingly small change in energy), there are reasons for continuing to study finite clusters as rough models of solids. Most particularly, a very high degree of self-consistency can be obtained in the electronic structure computations.

Recently, calculations for Fe and Ni clusters were performed by Lee and co-workers,[8–10] and, in general, good agreement with the bulk electronic structure, except for the spatial distribution of the spin density, was achieved. It is the aim of this paper to extend this approach to impurity systems, with the object of investigating the electronic structure of Fe, Co, and Ni impurities in copper metal. Our results are compared with experiments and with other calculations.

II. METHOD

Only a brief description of the method employed in these calculations is given below. For a complete description, see Refs. 8 and 9. The free-cluster calculations are performed on the basis of local-spin-density-functional theory by expanding the wave functions in an uncontracted Gaussian basis set of 14 s-, 9 p-, and 5 d-type functions. Including angular dependences, 66 independent functions per atom are used; however, extensive use of the cubic symmetry of the cluster keeps the problem to manageable size. The exponents of the orbital basis set are taken from the free-atom calculations performed by Wachters.[11]

In order to avoid the calculations of enormous numbers of two-electron integrals for the Coulomb matrix elements, we made an auxiliary fit to the charge density, using a separate Gaussian basis set of 14 s and 9 p functions

per atom. A variational fitting procedure was used, giving minimum errors in the electrostatic energy[12] instead of a least-squares fit to the charge density itself.

An exchange-correlation potential as parametrized by Rajagopal, Singhal, and Kimball[13] was used, and the corresponding matrix elements were calculated by direct numerical integration on a special three-dimensional grid developed for that purpose.[8]

The cluster densities of states (CDOS's) were obtained by broadening each eigenvalue with a Gaussian. Each state was decomposed by a Mulliken-population analysis, and the resulting l-like charges determine the width of the Gaussian used (0.6 eV for s and p types, 0.15 eV for d contributions) as well as the weights of the contribution to the CDOS.

III. RESULTS

A. Cu_{13}

A starting point for considering impurities in metals should be the electronic structure of the pure metal. Therefore, in Fig. 1 an energy-level diagram for a free Cu_{13} cluster in fcc geometry is shown. The nearest-neighbor distance of 4.83 a.u. corresponds to a Cu lattice constant of 6.83 a.u. We find that the Fermi energy coincides with a state of t_{2g} symmetry in accordance with previous calculations by Delley *et al.*[14] and Messmer *et al.*[15] using the discrete variation method and the $X\alpha$ scattered-wave method, respectively. This indicates that the assumed geometry presumably would not be stable with respect to a Jahn-Teller distortion. However, a detailed comparison with the level structure of Messmer *et al.* gives differences in both the ordering of levels of different symmetry (we find, for instance, that the first t_{1u} level is lower in energy than the first t_{2g} and e_g states, while the $X\alpha$ calculation predicts the t_{2g} and e_g states to be much lower than the t_{1u} state), as well as the total width of the occupied states ($E_{a_{1g}}-E_F=0.55$ versus 0.48 Ry in $X\alpha$) or the distance of the highest d states from the Fermi energy (0.04 versus 0.12 Ry in $X\alpha$). A Hartree-Fock study of Cu_{13} by Demuynck *et al.*[16] finds almost no overlap between the Cu $3d$ and $4s$ states and therefore predicts a completely different electronic structure than calculations based on local-density-functional theory.

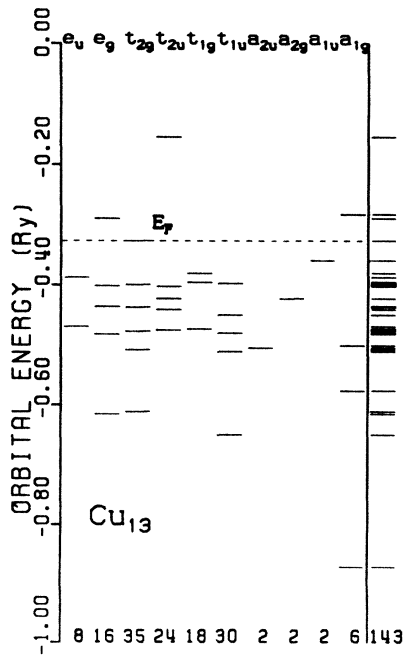

FIG. 1. Energy-level diagram for the Cu_{13} cluster. The symmetry and occupancy of these levels is also given. The dashed line indicates the Fermi energy.

A common way of comparing cluster and bulk calculations is a comparison of the density of states (DOS). Figure 2 shows the CDOS of the Cu_{13} cluster and, for comparison, the bulk fcc Cu DOS calculated by Bagayoko.[17] The overall agreement between these two calculations is very good; in particular, the four-peak structure of the bulk metal DOS originating from the Cu $3d$ bands embedded in the Cu $4s$ band is similar to that of the CDOS, as well as the total d-band width in the cluster and the bulk solid. However, the lowest of these four peaks in the CDOS is separated from the others, and the d band is shifted closer to the Fermi energy.

A Mulliken-population analysis gives for the central atom a $3d^{9.66}4s^{2.0}$ configuration and, for the shell atoms, $3d^{9.76}4s^{1.17}$. It must be noted that an allocation of the very delocalized $4s$ electrons to the different Cu sites is somewhat ambiguous, as some small negative $4s$ populations (and also some greater than 2) indicate.

The valence charge density is almost spherically symmetric around the nuclei as expected due to the full d shell and agrees quite well with valence densities obtained from an augmented-plane-wave (APW) band-structure calculation.[18] The $3d$ maximum has a value of 3.86 e/a.u.^{3} (3.79 e/a.u.^{3} in APW) and is located 0.33 a.u. (0.32 a.u.) away from the nucleus. The t_{2g}-e_g ratio of the d electron

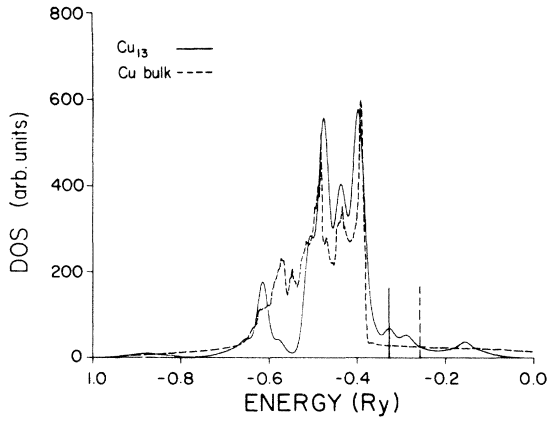

FIG. 2. Cluster density of states (CDOS) for the Cu_{13} cluster (solid line) and bulk Cu DOS (dashed line). In the CDOS states are broadened and weighted according to their l character in a Mulliken-population analysis (0.6 eV for s and p, 0.15 eV for d charges). The Fermi energies are indicated by a dashed (bulk) and a solid (cluster) straight line, and the bulk DOS is shifted in energy, so that the bulk and cluster $3d$ maxima coincide.

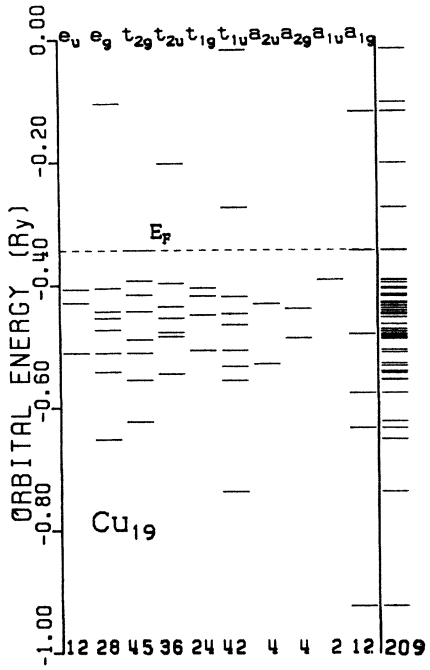

FIG. 3. Energy-level diagram for the Cu_{19} cluster.

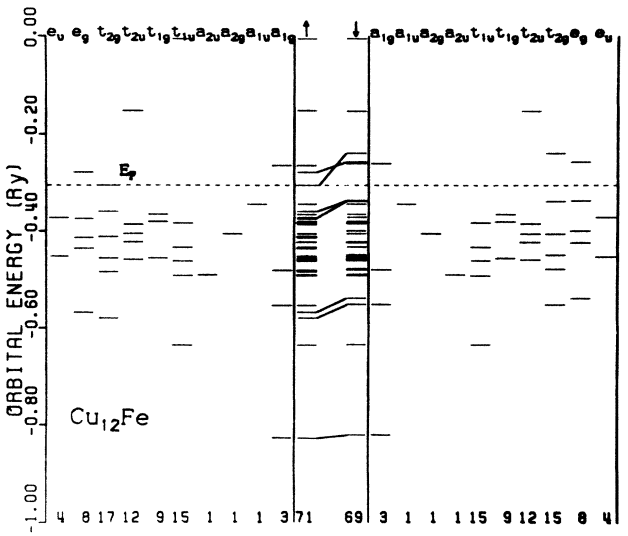

FIG. 4. Energy-level diagram for the $Cu_{12}Fe$ cluster (up- and down-spin states separated). In the summary some states of equal symmetry are connected by a line to indicate the amount of spin splitting.

populations of the central site is 1.48, a value which is near spherical symmetry (3:2).

B. Cu_{19}

It has been shown in the preceding section that even a Cu_{13} cluster can represent most of the electronic structure of bulk Cu. However, in order to get a more direct answer as to how the replacement of the central Cu by an magnetic impurity atom affects the electronic structure, we made calculations for Cu_{19} also. The energy-level diagram is shown in Fig. 3. There are again major differences between our and previous $X\alpha$ scattered-wave[3] results. For instance, we find at the Fermi energy two almost degenerate levels of a_{1g} and t_{2g} symmetry, while $X\alpha$ puts t_{2g} clearly below a_{1g}. Furthermore, we find the lowest t_{1u} state below the first t_{2g} and e_g states in contrast to the $X\alpha$ results. This brings our d-band width into close agreement with that of bulk Cu.

As can be seen from Table I, adding a second shell of Cu atoms leads to $3d$ populations, which are now largest at the center atom and not at the first shell as in Cu_{13}. Again, the CDOS of the center plus the first-shell atoms (Fig. 7) resembles the bulk Cu DOS very well, while the Cu_6 atoms form a "surface DOS" showing a single peak at relatively high energy. This surface DOS was also shown by Delley *et al.* on a Cu_{79} cluster.[14]

TABLE I. Mulliken-population analysis from integrated CDOS's (M stands for the central atom).

	$Cu_{12}Fe$	$Cu_{18}Fe$	$Cu_{18}Co$	$Cu_{18}Ni$	Cu_{19}
M sp ↑	1.00	1.15	1.09	1.04	1.14
M sp ↓	1.00	1.20	1.13	1.06	
M d ↑	4.45	4.87	4.89	4.89	4.94
M d ↓	2.20	1.82	2.84	4.20	
M tot	8.65	9.01	9.95	11.19	12.16
Cu_{12} sp ↑	0.60	0.64	0.65	0.66	0.61
Cu_{12} sp ↓	0.61	0.62	0.63	0.65	
Cu_{12} d ↑	4.87	4.87	4.87	4.85	4.88
Cu_{12} d ↓	4.87	4.83	4.84	4.84	
Cu_{12} tot	10.95	10.96	10.99	11.00	10.98
Cu_6 sp ↑		0.58	0.58	0.57	0.54
Cu_6 sp ↓		0.58	0.57	0.57	
Cu_6 d ↑		4.87	4.86	4.84	4.89
Cu_6 d ↓		4.87	4.86	4.83	
Cu_6 tot		10.90	10.87	10.81	10.86

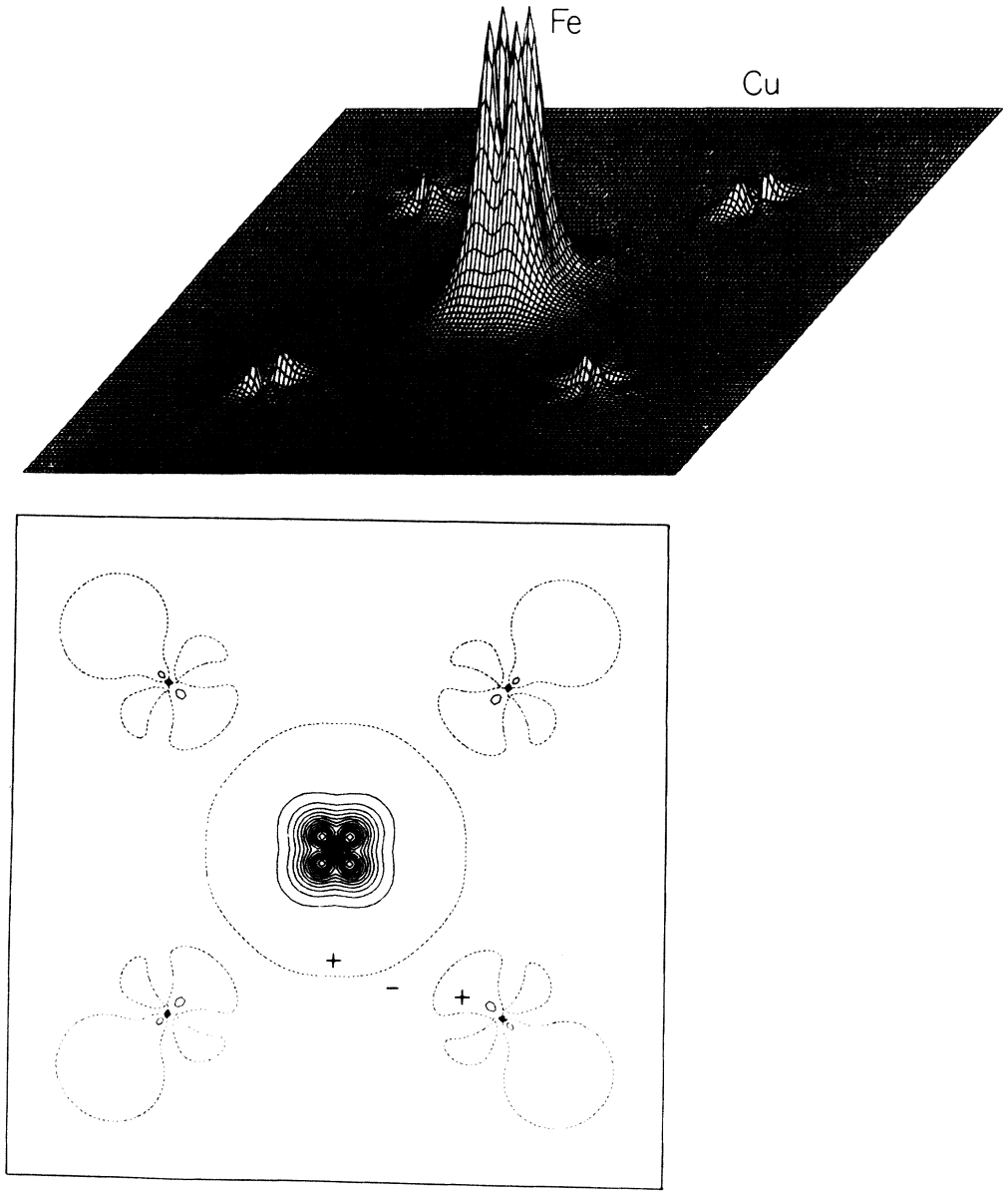

FIG. 5. Spin-density distribution of $Cu_{12}Fe$ in the (100) plane. Zero is at dashed lines; the contour intervals are at 0.05 e/a.u.^{3}. Positive and negative regions are labeled with + and −, the Fe $3d$ maxima are at 0.7 e/a.u.^{3}.

C. $Cu_{12}Fe$

When we replace the central Cu atom by Fe and allow spin polarization, an energy-level diagram (Fig. 4) indicates that the pure Cu states show almost no spin splitting, but the Fe d states are split by 20—67 mRy (0.27—0.91 eV) at the bottom and top of the "Cu d band." This splitting causes an excess of two spin-up electrons in a t_{2g} level. The exchange splitting of the Fe d states is substantially reduced compared with that of pure Fe clusters (Refs. 9 and 10) (0.7—3.1 eV) or bulk Fe (Ref. 19) (1.1—2.2 eV).

The spin density (Fig. 5) indicates the strong localization of the iron moment and the maxima point to the next Cu neighbors as expected from the level occupancy. The d electrons of Cu are also slightly positively spin polarized due to covalent interactions with Fe, but in the large "interstitial" region a small negative polarization occurs, indicating a dominance of spin-down $4s$ electrons. The spin densities at the nuclear sites of Fe and Cu are both negative (Table II), and the large value at Cu indicates the strong magnetic interaction in contrast with bulk-copper-like behavior. Note that in the valence-electron density an e_g dominance around the iron site is present, as one could see from the ratio of the t_{2g} electron number to that of e_g of 1.2.

The total magnetization of this cluster is $2\mu_B$, but a Mulliken analysis gives an Fe d moment of $2.2\mu_B$ which is partially screened by a negative polarization of 0.01 Cu $4s$ electrons (see Table I). This could be interpreted as a spin compensation cloud, as suggested by many experiments or theoretical approaches.[1,20,21]

TABLE II. Spin density at the nuclei (in e/a.u.^{3}).

	$Cu_{12}Fe$	$Cu_{18}Fe$	$Cu_{18}Co$	$Cu_{18}Ni$
M	−0.196	−0.224	−0.179	−0.100
Cu_{12}	−0.205	0.035	0.092	0.133
Cu_6		0.012	−0.027	−0.016

D. $Cu_{18}Fe$

In order to get a more realistic model of a single Fe impurity in Cu we add a second shell of Cu atoms to the cluster. This yields a level distribution as shown in Fig. 6(a). The Fermi level coincides with a partially occupied e_g spin-down level. This leads to a strong peak in the spin-down DOS (Fig. 7) and thus is consistent with de Haas–van Alphen measurements on dilute Cu-Fe, where resonance scattering occurs mainly at the minority states.[22,23] The total magnetization is $4\mu_B$, and the exchange splitting for Fe d states ranges from 20 mRy at the bottom to 90 mRy at the top (0.27–1.2 eV) of the occupied states. Our results disagree with $X\alpha$ scattered-wave results of Johnson *et al.*,[3] who find the Fermi energy at a t_{2g} spin-up level and claim that the exchange splitting is only 0.12–0.17 eV, and therefore a Jahn-Teller and/or a spin-orbit splitting of degeneracies could construct a nonmagnetic ground state at 0 K. Our exchange splitting is, however, in good agreement with that found by impurity calculations of Zeller, Dederichs, and coworkers.[4–7]

The total CDOS, which still resembles the bulk Cu DOS, could be partitioned into spin-up and spin-down Fe, Cu_{12}, and Cu_6 contributions (Fig. 7). The partial spin-up Fe CDOS is spread out over the entire Cu d band and is not restricted to a few eigenvalues. The spin-down Fe CDOS is strongly reduced and shifted to higher energies and shows a relative strong resonance at the Fermi energy. These facts are in good agreement with the impurity calculations mentioned above, although these authors find an additional well-defined sharp spin-up virtual bound state. Since our Fe spin-up d states are much more hybridized with Cu d than the spin-down Fe d states, it is obvious that we cannot find such a resonance. Furthermore, such sharp resonances are not detected in Cu-Fe by means of x-ray photoemission spectroscopy,[24] where only a smooth enhancement in the s,p region above the Cu d band was found. However, such virtual bound states were found experimentally in Ag-Mn (Ref. 24) and also in cluster calculations of Ag-Fe (Ref. 25), i.e., in cases where the host and the impurity d states do not fall into the same energy range. In addition, Cohen and Slichter[26] performed model calculations for $3d$ impurities in Cu, fitting experimental NMR satellite data. These authors find a peak only in the spin-down Fe DOS, which is located at the Fermi energy, but no spin-up resonance. (Note, that spin-up and spin-down are exchanged in their paper.) The Cu_{12} CDOS resembles bulk Cu, both in spin-up and spin-down, and the Cu_6 CDOS shows a single peak at relatively high energy corresponding to a surface DOS.

One can see from Table I that the total moment of $4\mu_B$ is not located only at the Fe atom, but that also the Cu_{12}

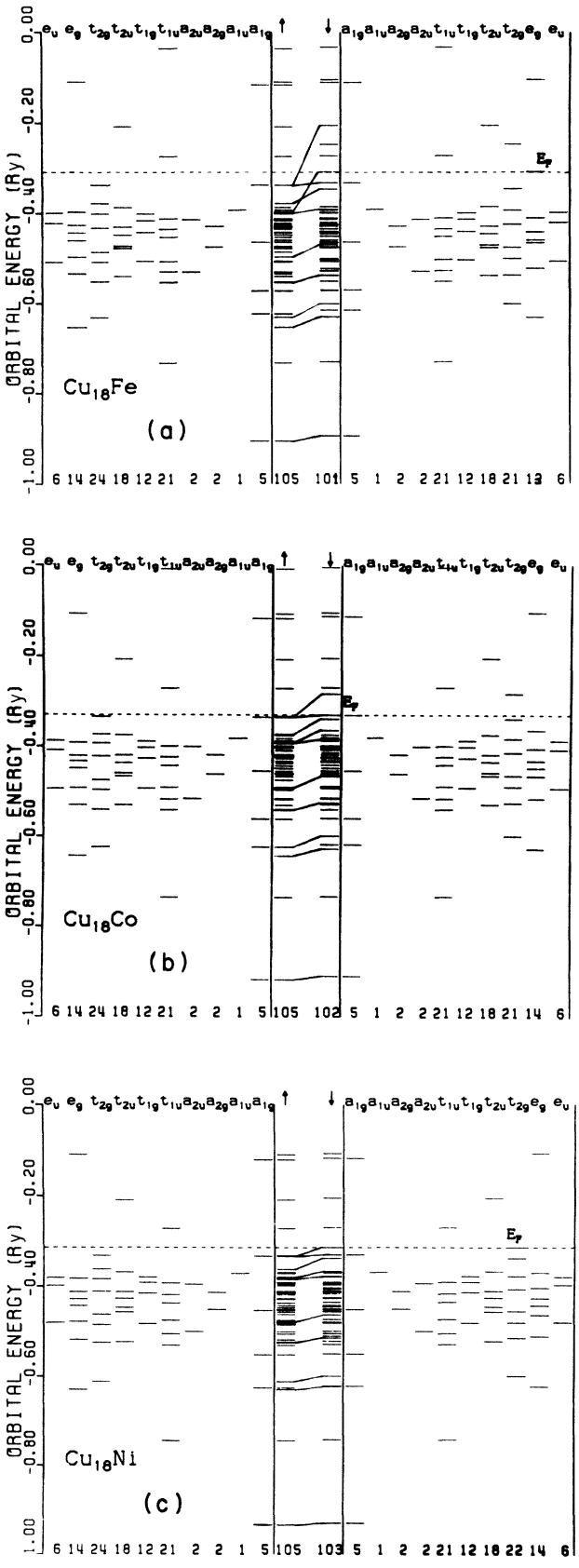

FIG. 6. Energy-level diagram for 19-atom clusters: (a) $Cu_{18}Fe$, (b) $Cu_{18}Co$, and (c) $Cu_{18}Ni$.

atoms show a slight ferromagnetic $3d$ polarization in agreement with the recent cluster-impurity calculation.[6] The pure Fe d moment of $3.05\mu_B$ is in good agreement with experimental data found by neutron-diffraction measurements[21,27] or susceptibility measurements by Steiner *et al.*[28] and much larger than that of bulk Fe (Ref. 19) ($2.16\mu_B$). Again a small "spin compensation cloud" can be seen (Fe $4s,p$ and Cu $4s,p$ contributions are indistinguishable) and the Cu_6 atoms are almost unpolarized.

The negative polarization in the spin density (Fig. 8) is spatially reduced due to the additional moment of the Cu_{12} atoms, while on the Cu_6 atoms almost no polarization is present. On the iron nucleus there is a strong negative spin density of -0.224 e/au.^{3}, which could be compared to the bulk Fe contact spin density[19] of -0.406 e/a.u.^{3}, while the Cu sites, in contrast to the $Cu_{12}Fe$ cluster, show only small and positive spin densities. In this $Cu_{18}Fe$ cluster we find no indication of oscillatory

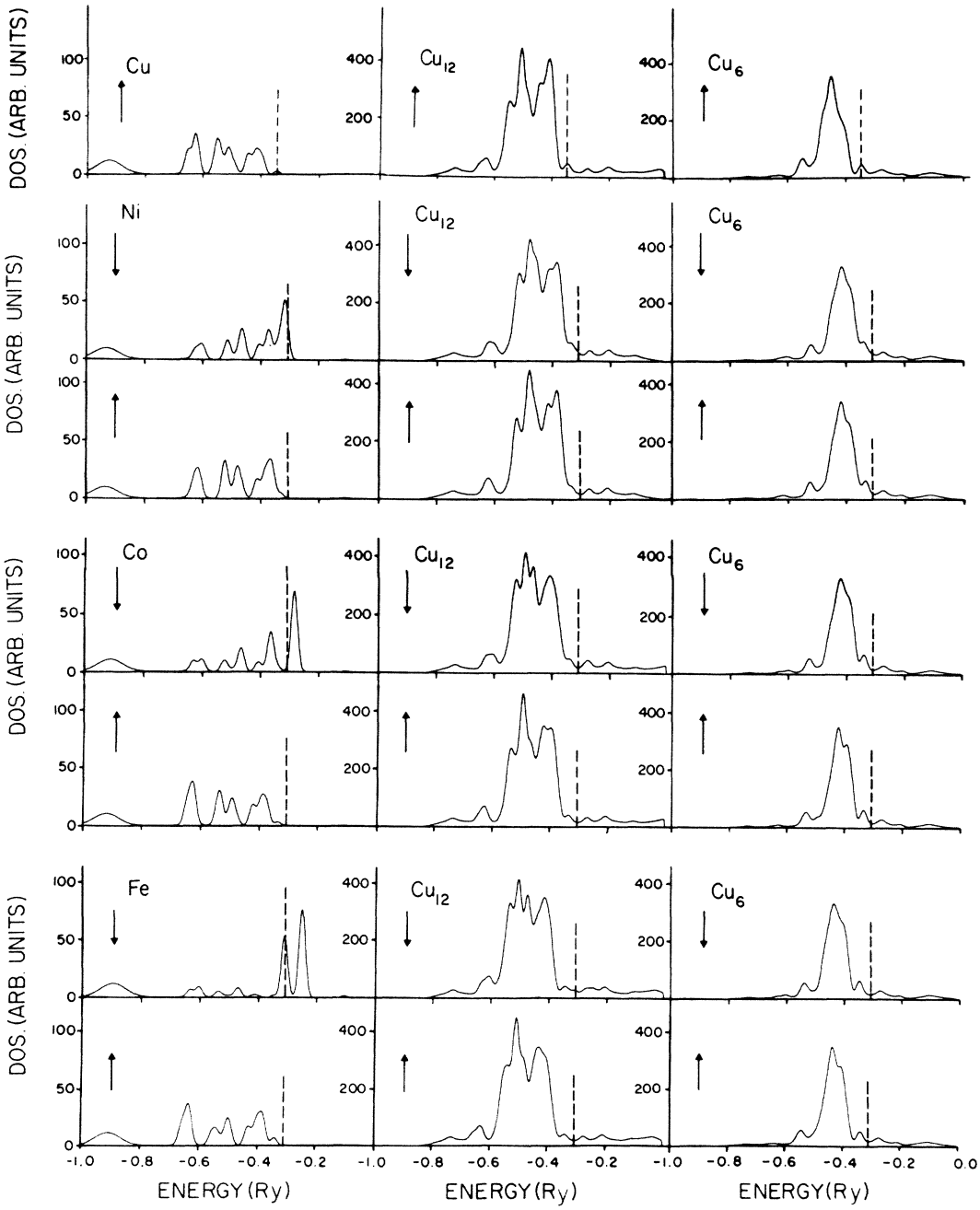

FIG. 7. Spin-up and spin-down local partial cluster density of states for (a) Cu_{19} (spin-up only), (b) $Cu_{18}Ni$, (c) $Cu_{18}Co$, and (d) $Cu_{18}Fe$. Note the different scales for the DOS of the center and the shell atoms.

behavior of the spin densities at the first and second shell of Cu atoms, as one would expect from Knight-shift measurements[20] or model calculations.[26] In the valence density (Fig. 9) the dominance of e_g symmetry around Fe as well as the relative strong deviation from spherical symmetry in the $3d$ density of the "surface atoms" Cu_6 is obvious. The latter indicates, together with the partial CDOS of the Cu_6 atoms (Fig. 7), a relative strong "cluster effect" on the electronic properties of atoms in such a cluster with free boundaries, and suggests an increase of the cluster size (additional shells) or the use of proper boundary conditions in order to obtain results in better agreement with the solid.

E. $Cu_{18}Co$

Our calculation for this cluster yields a total magnetic moment of $3\mu_B$ and a level structure shown in Fig. 6(b). Again, the Fermi energy falls on a spin-down state (a_{1g}), but t_{2g} and a_{1g} states are very close together at E_F. The exchange splitting of the predominantly Co states is reduced in comparison with those of Fe in the $Cu_{18}Fe$ cluster to about 20—50 mRy, in accordance with de Haas—van Alphen measurements.[22] Single-impurity calculations by Podloucki *et al.*[4] originally found Co to be nonmagnetic. However, in a recent improvement of their method, now including now only the single impurity but also the first Cu neighbors in the self-consistent process, their Co cluster also becomes ferromagnetic.[6]

The partial CDOS is shown in Fig. 7. It is obvious that there is no significant difference in the Cu_{12} and Cu_6 partial CDOS between $Cu_{18}Fe$ and $Cu_{18}Co$. The Fermi energy falls now between the two characteristic impurity spin-down peaks (a_{1g} level), whereas in the Fe cluster it was at the lower one.

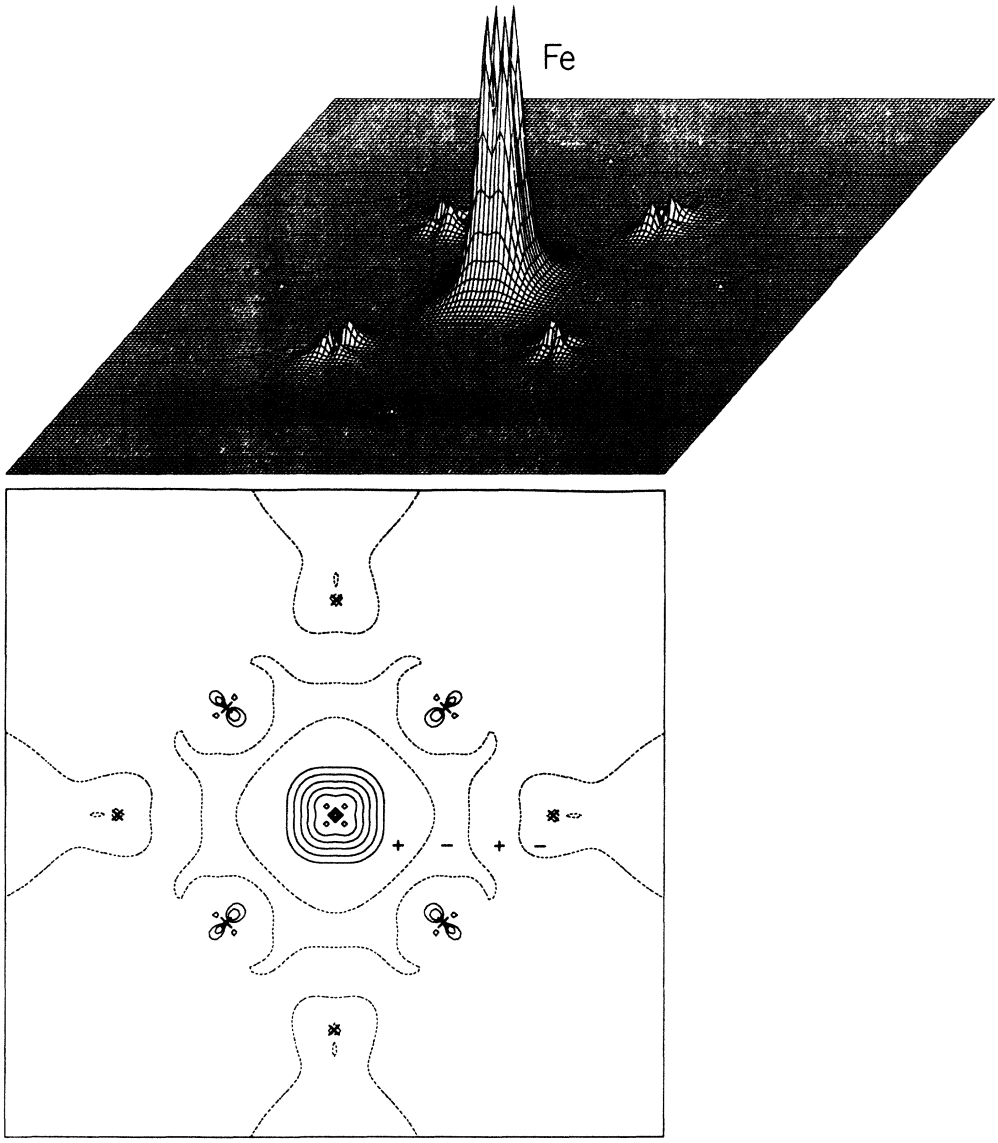

FIG. 8. Spin-density distribution of $Cu_{18}Fe$ in the (100) plane. Zero is dashed lines, the lowest contour is 0.025 e/a.u.^{3}, and adjacent lines differ by a factor of 2. The Fe $3d$ maxima are at 0.9 e/a.u.^{3}. The position of the Cu nuclei are indicated by crosses.

The total magnetic moment of the cluster is $3\mu_B$, while the Co has a local moment of only $2\mu_B$. Again, a negative polarization of the conduction electrons can be seen, and the neighboring Cu atoms show a slight ferromagnetic polarization of $0.03\mu_B$ (Table I). These facts are in qualitative agreement with Ref. 6, but these authors find only $0.96\mu_B$ at the Co site. However, since the inclusion of the first Cu shell increased their magnetic moment from 0 to nearly $1\mu_B$, further improvements may again change the absolute value, especially since our second-shell atoms also became slightly magnetic in contrast to $Cu_{18}Fe$.

The spin density around Co shows an even stronger t_{2g} symmetry than that around Fe, since now almost all spin-up excess comes from a t_{2g} level. There is again a negative spin density between the local moment and the Cu neighbors, and the Cu_6 atoms participate more strongly in the magnetic interaction than in the Fe case (Fig. 10). The spin densities on the Cu_{12} and Cu_6 sites show opposite signs and the magnitude on the Cu_6 atoms is much smaller. This is in contrast to our $Cu_{18}Fe$ results

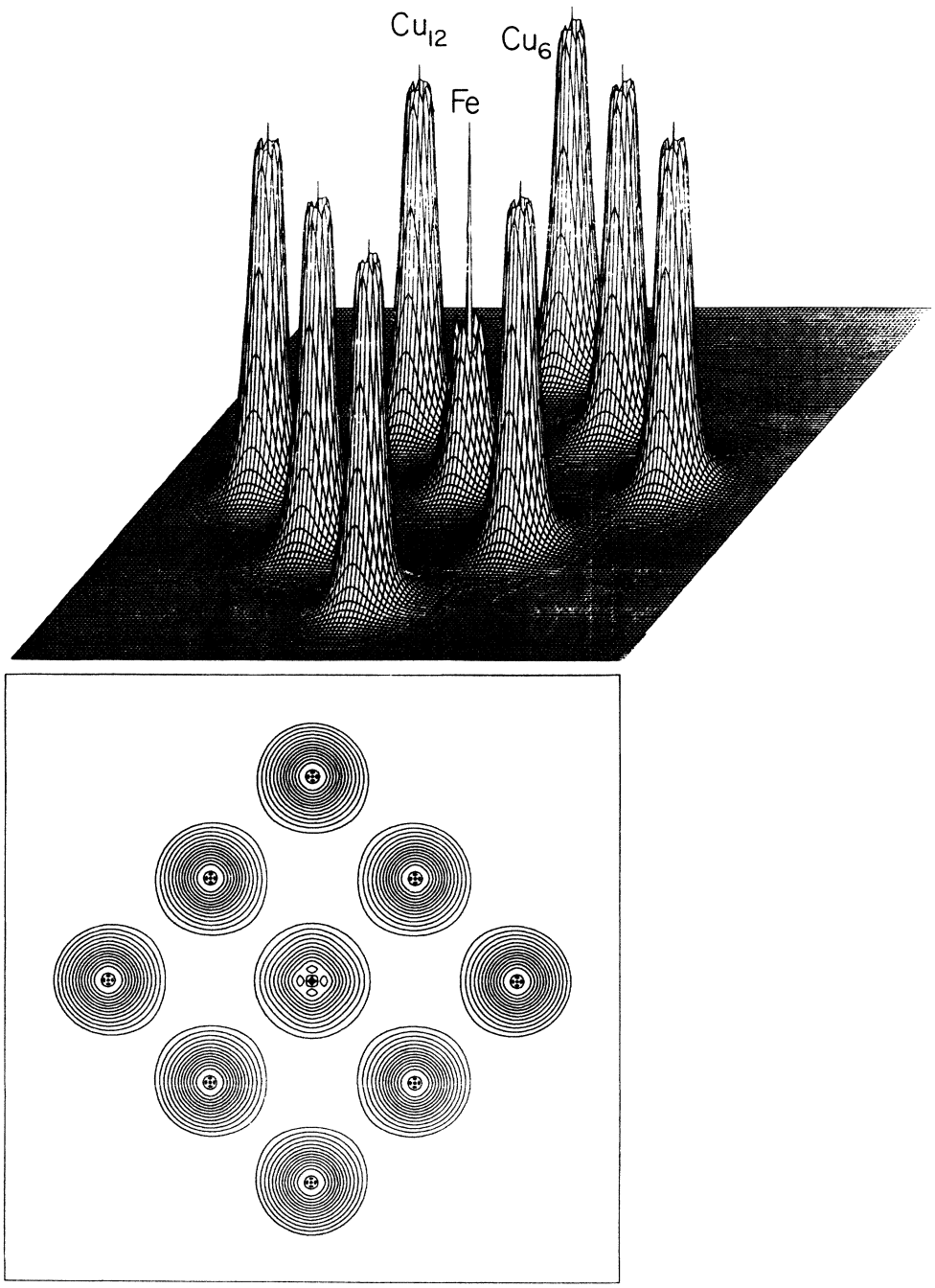

FIG. 9. Valence-electron density of $Cu_{18}Fe$ in the (100) plane. The lowest contour is at 0.05 e/a.u.^{3}; adjacent lines differ by a factor of $\sqrt{2}$. The Fe $3d$ maxima are at 1.9 e/a.u.^{3} and the Cu $3d$ maxima are at 3.9 e/a.u.^{3}.

(Table II); however, these findings may depend strongly on the cluster size.

F. $Cu_{18}Ni$

The experimental situation for Ni impurities in Cu is the most unclear one. It is generally believed that no strong localized magnetic moment exists. However, from NMR data[29,30] a small permanent moment can be deduced, and many authors suggest consideration of spin fluctuations.[31]

Our spin-polarized calculation finds the electronic structure displayed in Fig. 6(c) and a total magnetic moment of $2\mu_B$. The Fermi energy coincides with a singly occupied t_{2g} down state, and it is obvious that a slight shift of the spin-up and spin-down a_{1g} states to higher energies (20 mRy) would produce a nonmagnetic cluster. However, the electronic structure in a non-spin-polarized scattered-wave calculation[11] does not agree either with our results for the ordering of levels of different symmetry or in regard to the total width of the occupied valence states ($E_F - E_{a_{1g}} = 0.62$ Ry versus 0.44 Ry in $X\alpha$). Our exchange splitting is further reduced to about 10—24 mRy.

The partial CDOS in Ni (Fig. 7) shows, as do the occupancies in Table I, that almost all Ni states are now below E_F and it is therefore reasonable that x-ray photoemission spectroscopy measurements[24] found the strongest impurity resonances for Ni in the Fe,Co,Ni series.

In this highly correlated system, even the second-nearest-neighbor Cu_6 atoms show, remarkably, ferromagnetic aligned $3d$ moments. The local Ni moment is reduced to less than $0.7\mu_B$ and is quite comparable to that of bulk Ni (Ref. 32) ($0.57\mu_B$). For that purpose it is also reasonable that the contact spin density of -0.100 e/a.u.^{3} is close to the bulk value of -0.110 e/a.u.^{3}. The spin density around the Ni site shows predominantly t_{2g} character (Fig. 11). The spin density at the Cu_{12} site is remarkably high (Table II) and indicates again the high correlation of magnetic interactions in the Cu-Ni system.

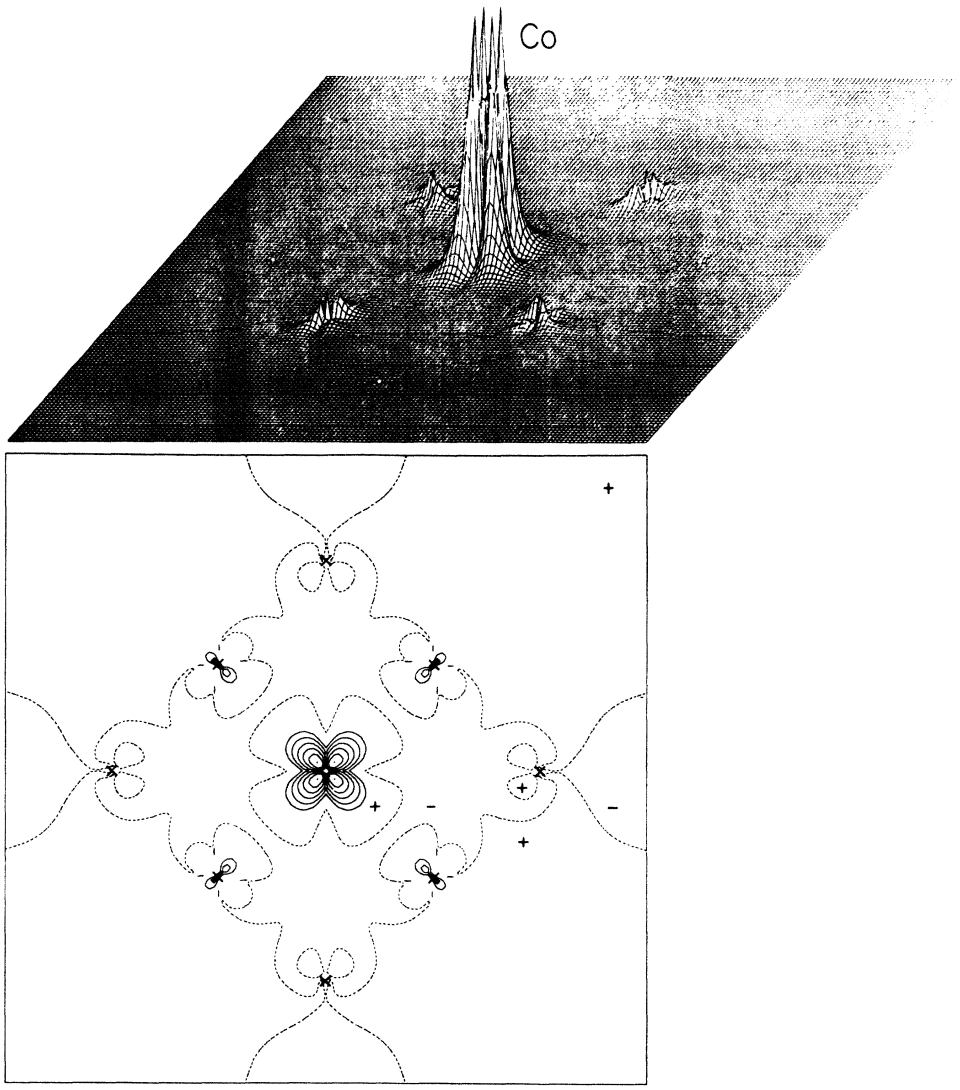

FIG. 10. Spin-density distribution of $Cu_{18}Co$ in the (100) plane. The Co $3d$ maxima are at 0.8 e/a.u.^{3}.

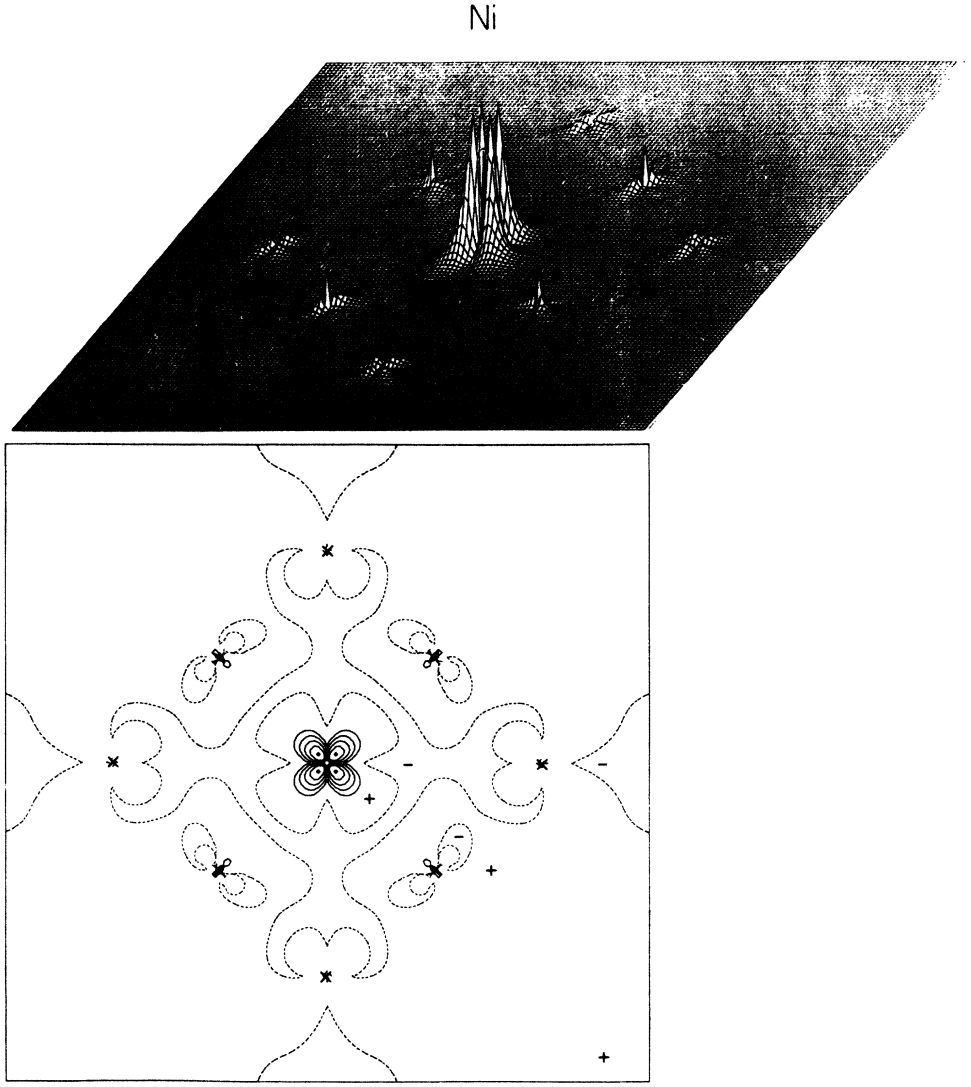

FIG. 11. Spin-density distribution of $Cu_{18}Ni$ in the (100) plane. The Ni $3d$ maxima are at 0.46 e/a.u.^{3}.

IV. SUMMARY

We have performed spin-polarized self-consistent-field cluster calculations based on local-spin-density-functional theory for Cu_{13}, $Cu_{12}Fe$, Cu_{19}, $Cu_{18}Fe$, $Cu_{18}Co$, and $Cu_{18}Ni$ with free boundaries using an expansion of the wave functions into Gaussian orbitals.

Our results are generally in disagreement with that obtained by the $X\alpha$ scattered-wave method,[3,15] but agree reasonably with discrete-variation-method calculations[14] for Cu_{13}. The Cu d band is completely embedded in the $4s$ band as in bulk copper, whereas a Hartree-Fock calculation did not find this complete overlap between s and d states. Our CDOS for Cu_{13}, as well as for the Cu_{12} shell in the impurity systems, resembles that of bulk Cu. Furthermore, the CDOS of the Cu_6 shell is very similar to that obtained for the surface atoms on a Cu_{79} cluster.[14] Since the valence-electron density of the central site also agrees quite well with that of an augmented-plane-wave calculation,[18] it is obvious that the electronic structure of a Cu_{13} cluster already resembles that of the bulk.

For that reason it was reasonable, after including an additional Cu shell, to study magnetic impurities like Fe, Co, and Ni in Cu. Our results for $Cu_{18}Fe$ are again in contradiction to $X\alpha$ scattered-wave calculations,[3] but agree well, at least for Fe and Co, with impurity calculations by a Green's-function method.[6] The total moments of the $Cu_{18}Fe$, $Cu_{18}Co$, and $Cu_{18}Ni$ clusters are those of the free atoms, but the spin distribution is different. Some of the moment becomes delocalized and spread out over the Cu atoms. The spin splitting of the Fe impurity is reduced by a factor of 2 in comparison with bulk Fe, the local magnetic moment of $3.05\mu_B$ is in excellent agreement with neutron-diffraction[27] or Mössbauer[28] experiments, and de Haas–van Alphen[22] measurements found mainly spin-down scattering at the Fermi energy in accordance with our results. We find a region of negative spin density, mainly from the conduction electrons, and a slight ferromagnetic polarization of the first shell of Cu neighbors, whereas the second-shell atoms are nearly po-

larization free. These facts, as well as cluster studies of other impurity systems,[25,33,34] clearly contradict the statement in Refs. 4 and 5 that cluster calculations cannot yield reasonable results for impurities.

In the Co and Ni cases the agreement with these recent Green's-function calculations is not as good and indicates that both exact treatment of short-range-order interactions (cluster approach) and proper treatment of long-range effects (Green's-function method) could be important in these systems. For instance, for the Co impurity system the treatment of a single impurity in an otherwise unperturbed Cu host was clearly insufficient and yielded a nonmagnetic state. Inclusion of some short-range interactions causes Co to flip into a magnetic state. On the other hand we cannot exclude that a third Cu shell or proper boundaries will affect our results for the Ni impurity in a way that a further reduction or even a complete disappearance of magnetism will occur, especially because we observe a high correlation of the magnetic effects on Ni and the first and second shell of Cu atoms. While the spin densities at the impurity nuclei decrease as expected in the Fe,Co,Ni series, a drastic increase was found at the first-shell Cu_{12} atoms. The spin densities at the Cu_6 atoms are always smaller in magnitude, but their signs do not show any systematic trend. For the Co and Ni clusters the oscillatory behavior is in agreement with Knight-shift measurements.[26]

ACKNOWLEDGMENT

This work was supported by the U.S. Army Research Office and Contract No. DAAG29-85-K-0036.

[1]A. J. Heeger, in *Solid State Physics,* edited by H. Ehrenreich, F. Seitz, and D. Turnbull (Academic, New York, 1969), Vol. 23.
[2]J. Kondo, in *Solid State Physics,* Ref. 1.
[3]K. H. Johnson, D. D. Vvedensky, and R. P. Messmer, Phys. Rev. B **19**, 1519 (1979).
[4]R. Podlucki, R. Zeller, and P. H. Dederichs, Phys. Rev. B **22**, 5777 (1980).
[5]R. Zeller, R. Podloucki, and P. H. Dederichs, Z. Phys. B **38**, 165 (1980).
[6]P. J. Braspenning, R. Zeller, A. Lodder, and P. H. Dederichs, Phys. Rev. B **29**, 703 (1984).
[7]A. Oswald, R. Zeller, P. J. Braspenning, and P. H. Dederichs, J. Phys. F **15**, 193 (1985).
[8]K. Lee, Ph.D. thesis, Louisiana State University, 1984 (unpublished) (available from University Microfilms International, Ann Arbor, MI 48106).
[9]K. Lee, J. Callaway, and S. Dhar, Phys. Rev. B **30**, 1724 (1984).
[10]K. Lee, J. Callaway, K. Kwong, R. Tang, and A. Ziegler, Phys. Rev. B **31**, 1796 (1985).
[11]A. J. H. Wachters, J. Chem. Phys. **52**, 1033 (1970).
[12]J. W. Mintmire and B. W. Dunlap, Phys. Rev. A **25**, 88 (1983).
[13]A. K. Rajagopal, S. P. Singhal, and J. Kimball (unpublished), quoted by A. K. Rajagopal, in *Advances in Chemical Physics,* edited by G. I. Prigogine and S. A. Rice (Wiley, New York, 1979), Vol. 41, p. 59.
[14]B. Delley, D. E. Ellis, A. J. Freeman, E. J. Baerends, and D. Post, Phys. Rev. B **27**, 2132 (1983).
[15]R. P. Messmer, S. K. Knudson, K. H. Johnson, J. B. Diamond, and C. Y. Yang, Phys. Rev. B **13**, 1396 (1976).
[16]J. Demuynck, M. Rohmer, A. Strick, and A. Veillard, J. Chem. Phys. **75**, 3443 (1981).
[17]D. Bagayoko, Int. J. Quantum. Chem. **17**, 527 (1983).
[18]J. Redinger (private communication); J. Redinger, K. Schwarz, N. K. Hansen, G. E. W. Bauer, and J. R. Schneider (unpublished).
[19]J. Callaway and C. S. Wang, Phys. Rev. B **16**, 2095 (1977).
[20]J. Boyce and C. P. Slichter, Phys. Rev. B **13**, 379 (1976).
[21]M. H. Dickens, C. G. Shull, W. C. Koeler, and R. M. Moon, Phys. Rev. Lett. **35**, 595 (1975).
[22]P. T. Coleridge, G. B. Scott, and I. M. Templeton, Can. J. Phys. **50**, 1999 (1972).
[23]H. Alles, R. J. Higgins, and D. H. Lowndes, Phys. Rev. Lett. **30**, 705 (1973).
[24]H. Hochst, P. Steiner, and S. Hufner, Z. Phys. B **38**, 201 (1980).
[25]B. Delley, D. E. Ellis, and A. J. Freeman, J. Magn. Magn. Mater. **30**, 71 (1982).
[26]J. D. Cohen and C. P. Slichter, Phys. Rev. B **22**, 45 (1980).
[27]J. R. Davis and T. J. Hicks, J. Phys. F **9**, L7 (1979).
[28]P. Steiner, S. Hufner, and W. V. Zdrojewsky, Phys. Rev. B **10**, 4704 (1974).
[29]R. Nevald and G. Petersen, J. Phys. F **5**, 1778 (1975).
[30]D. C. Lo, D. V. Lang, J. B. Boyce, and C. P. Slichter, Phys. Rev. B **8**, 973 (1973).
[31]D. Beaglehole, Phys. Rev. B **14**, 341 (1976).
[32]C. S. Wang and J. Callaway, Phys. Rev. B **15**, 298 (1977).
[33]A. Rodriguez and J. Keller, J. Phys. F **11**, 423 (1981).
[34]D. Guenzburger and D. E. Ellis, Phys. Rev. B **31**, 93 (1985).

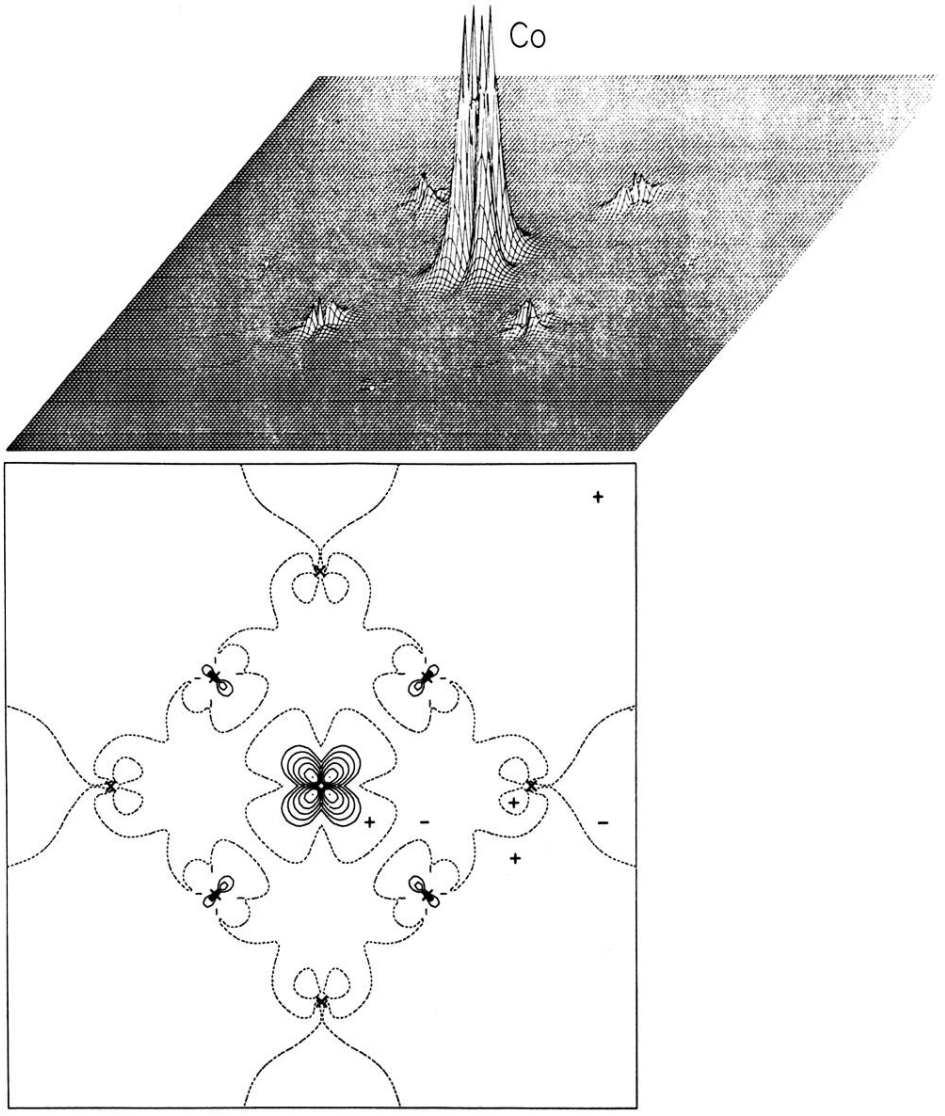

FIG. 10. Spin-density distribution of $Cu_{18}Co$ in the (100) plane. The Co $3d$ maxima are at 0.8 e/a.u.^{3}.

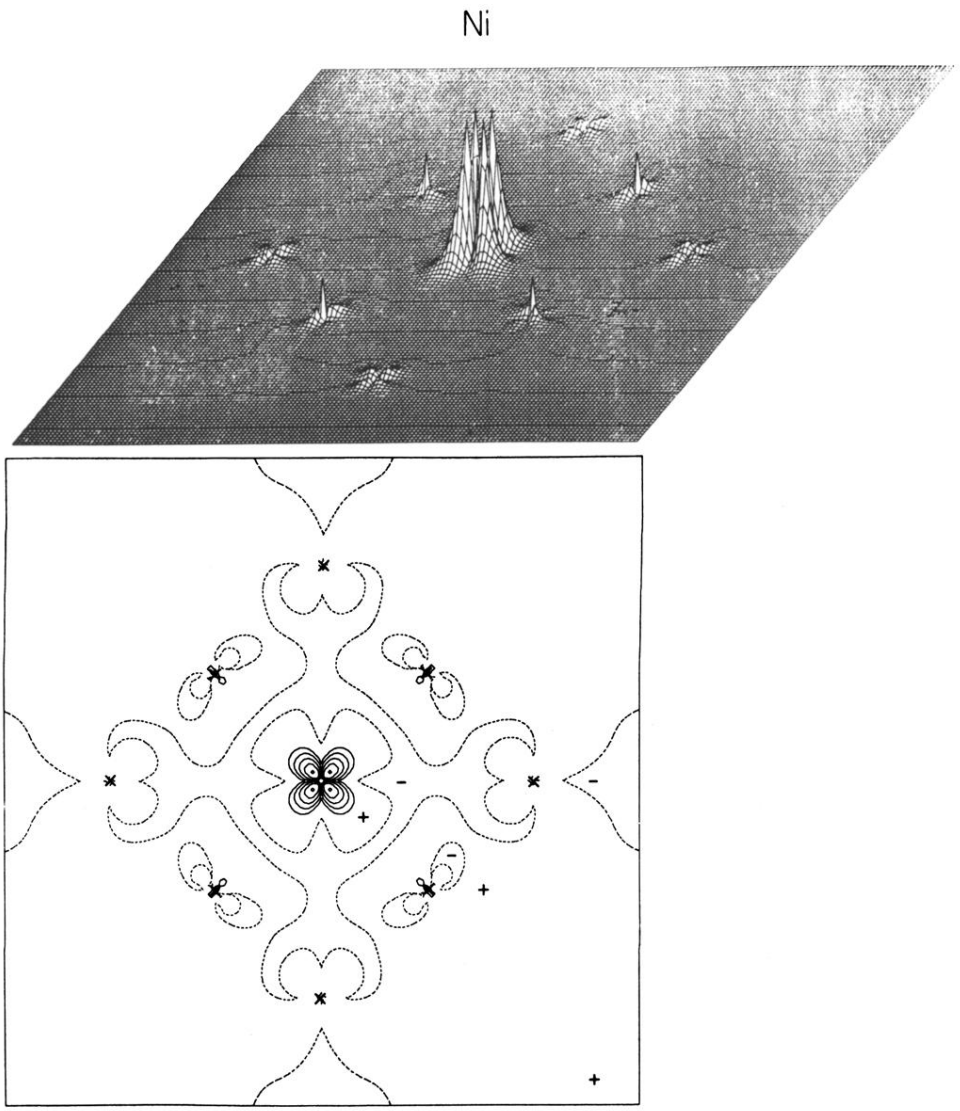

FIG. 11. Spin-density distribution of $Cu_{18}Ni$ in the (100) plane. The Ni $3d$ maxima are at 0.46 e/a.u.^{3}.

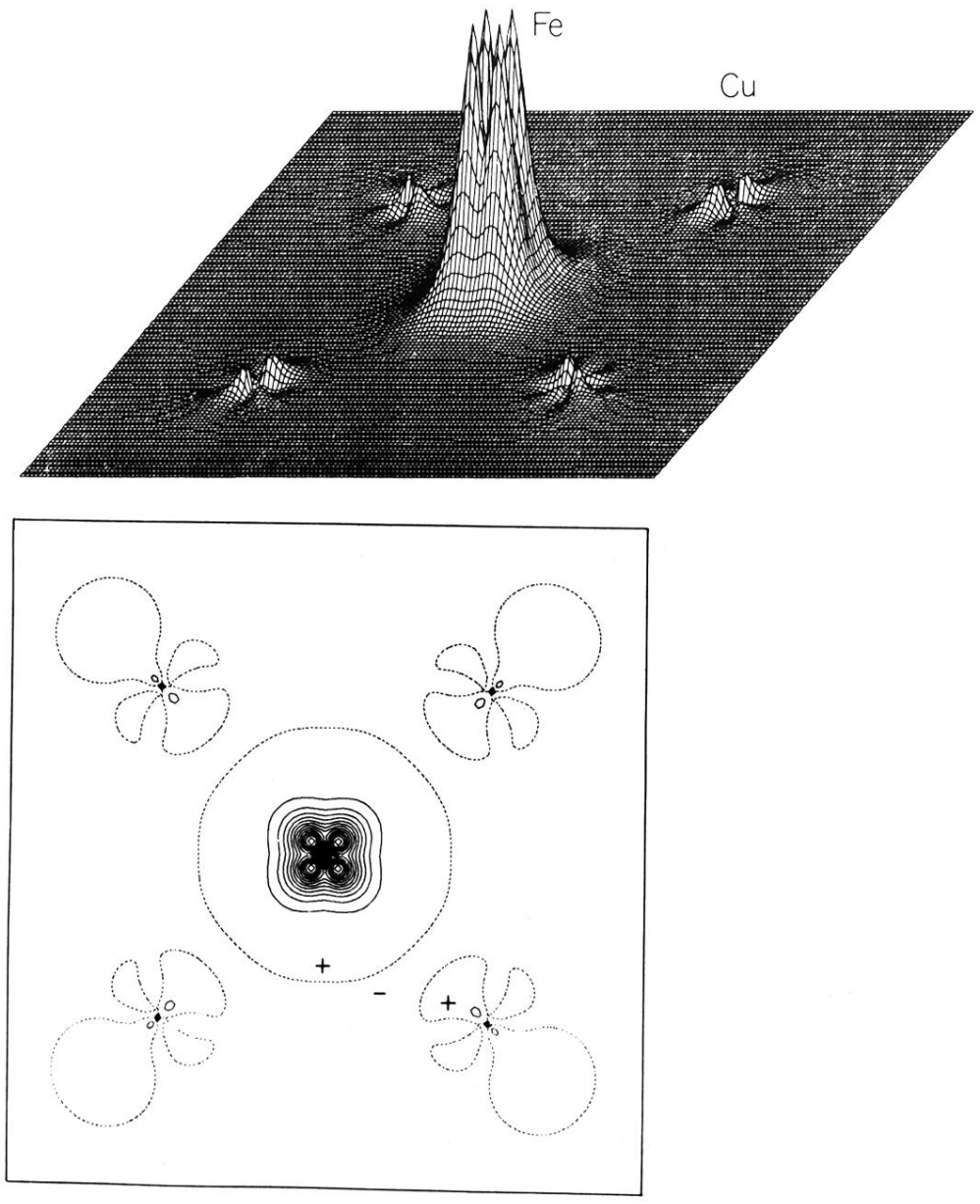

FIG. 5. Spin-density distribution of $Cu_{12}Fe$ in the (100) plane. Zero is at dashed lines; the contour intervals are at 0.05 e/a.u.^{3}. Positive and negative regions are labeled with + and −, the Fe 3d maxima are at 0.7 e/a.u.^{3}.

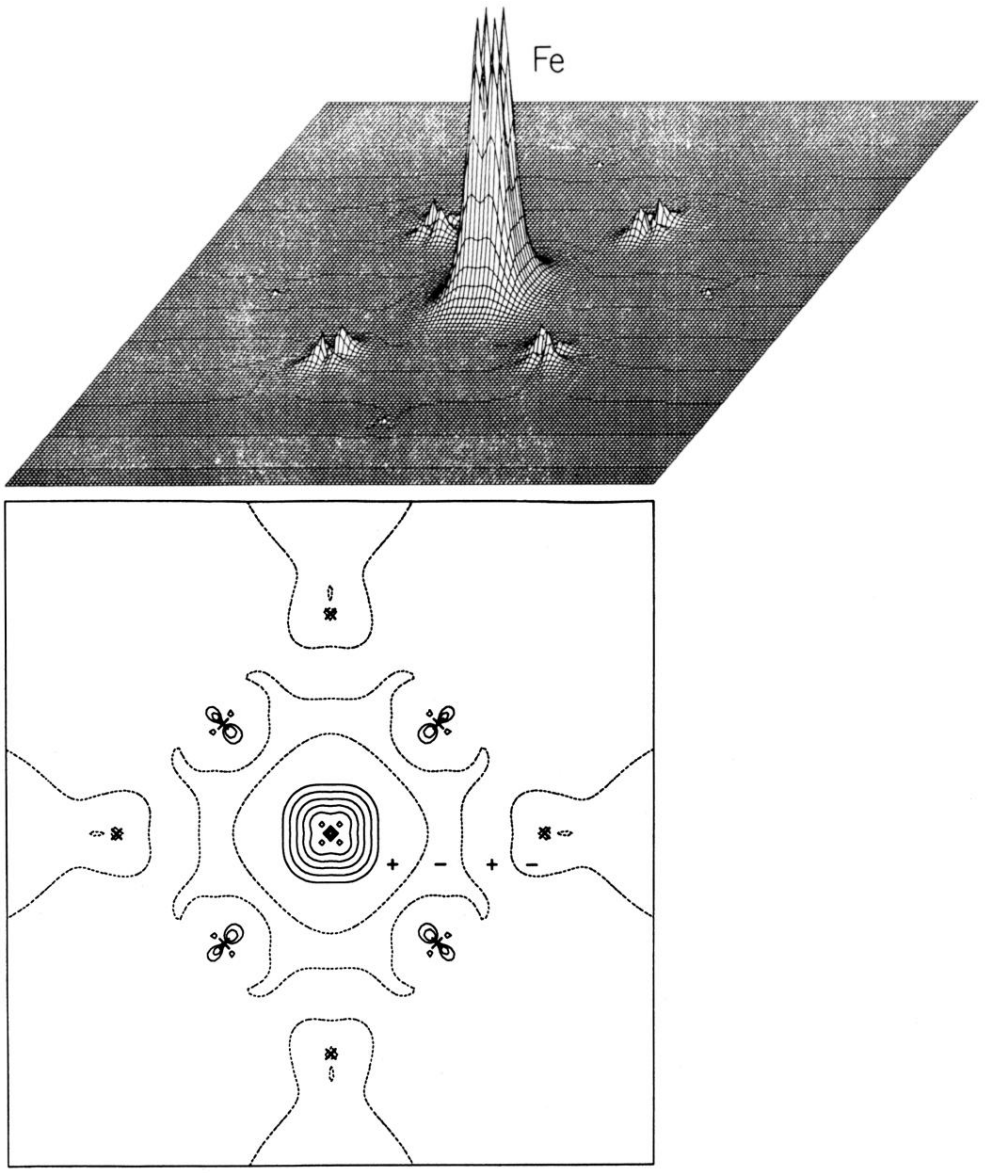

FIG. 8. Spin-density distribution of $Cu_{18}Fe$ in the (100) plane. Zero is dashed lines, the lowest contour is 0.025 e/a.u.^{3}, and adjacent lines differ by a factor of 2. The Fe $3d$ maxima are at 0.9 e/a.u.^{3}. The position of the Cu nuclei are indicated by crosses.

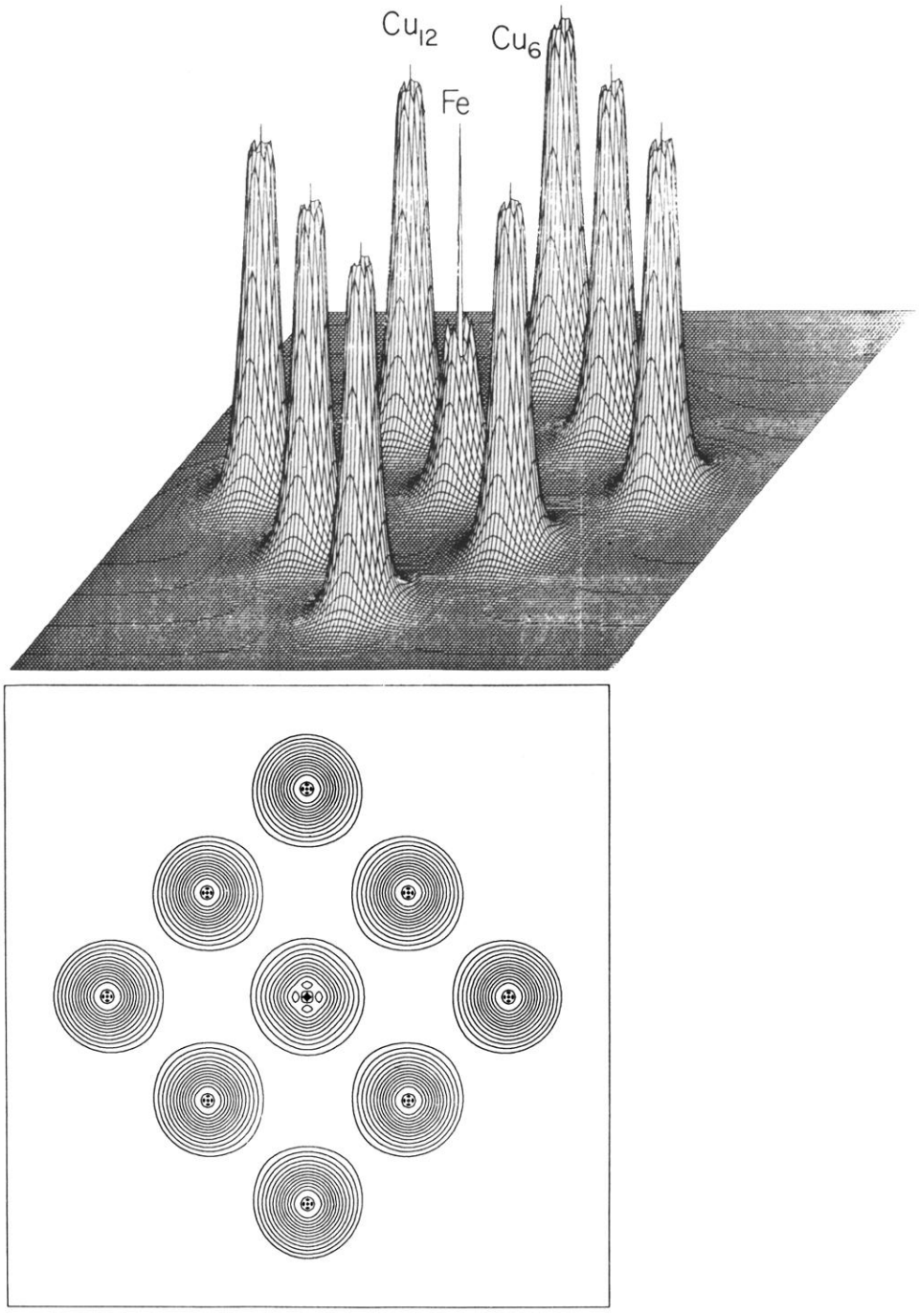

FIG. 9. Valence-electron density of $Cu_{18}Fe$ in the (100) plane. The lowest contour is at 0.05 e/a.u.^{3}; adjacent lines differ by a factor of $\sqrt{2}$. The Fe $3d$ maxima are at 1.9 e/a.u.^{3} and the Cu $3d$ maxima are at 3.9 e/a.u.^{3}.